

## Biexcitons in Semiconductor Quantum Dots

Y. Z. Hu,<sup>(1)</sup> S. W. Koch,<sup>(1,2)</sup> M. Lindberg,<sup>(2)</sup> N. Peyghambarian,<sup>(2)</sup> E. L. Pollock,<sup>(3)</sup>  
and Farid F. Abraham<sup>(4)</sup>

<sup>(1)</sup>Department of Physics, University of Arizona, Tucson, Arizona 85721

<sup>(2)</sup>Optical Sciences Center, University of Arizona, Tucson, Arizona 85721

<sup>(3)</sup>Lawrence Livermore National Laboratory, University of California, Livermore, California 94550

<sup>(4)</sup>IBM Research Division, Almaden Research Center, 650 Harry Road, San Jose, California 95120

(Received 27 December 1989)

Theoretical and experimental results are reported which provide the first evidence for biexciton states in semiconductor quantum dots. The theory predicts an increasing biexciton binding energy with decreasing dot size. Unlike bulk semiconductors, quantum dots have excited biexciton states which are stable. These biexciton states are observed as pronounced induced absorption features on the high-energy side of the bleached exciton resonances in femtosecond and nanosecond pump-probe experiments of quantum dots in glass matrices.

PACS numbers: 71.35.+z, 78.20.Dj

In contrast to bulk semiconductors, where even the ground-state resonance of the biexciton (two-electron-hole-pair state) can be detected only in materials with a relatively large band gap,<sup>1</sup> we predict that energetically higher two-pair states in quantum dots are observable quite easily as increasing probe absorption on the high-energy side of the exciton (one-electron-hole pair) resonances. Since the excited states of the biexciton are typically unbound in bulk semiconductors, their appearance in quantum dots is a unique consequence of the spatial confinement in such systems.

For simplicity, we present our calculations for the case of intrinsic semiconductor quantum dots, but additional investigations show that the predicted features are quite universal and even enhanced in systems with imperfections, such as charged impurities or traps. We compare the theoretical results with our femtosecond and nanosecond pump-probe experiments of CdS and CdSe quantum dots in glass matrices. The experiments clearly show the predicted induced absorption features in addition to the bleaching of the inhomogeneously broadened exciton resonance.

The quantum dots are modeled as dielectric spheres with perfect confinement of the optically generated electron-hole pairs.<sup>2,3</sup> As in Ref. 4, we expand the wave functions of the exciton and biexciton states in terms of the eigenfunctions of the noninteracting electron-hole system. The expansion is truncated after  $M$  terms, and  $M$  is increased until satisfactory convergence is ensured. The kinetic-energy terms are diagonal in the chosen basis and the Coulomb matrix elements are evaluated numerically. The resulting matrices for the one- and two-pair Hamiltonians are diagonalized numerically to yield the eigenfunctions and eigenvalues of the system. To improve the convergence of the procedure, we use the fact that the exciton and biexciton states are eigenfunctions of the total angular momentum operator and its  $z$

component. We start with a relatively small number,  $M \cong 40$ , of basis functions and successively increase  $M$  until the lowest-energy eigenvalues converge to within a few percent. Typically, we use a few hundred eigenfunctions for the final results.

In Fig. 1, we plot the ground-state biexciton binding energy,

$$\delta E_2 = 2E_1 - E_2, \quad (1)$$

as function of the radius  $R$  of the quantum dots (solid line). Here,  $E_1$  and  $E_2$  are the exciton and biexciton ground-state energies, respectively. To eliminate most of the material-parameter dependencies, we scale all energies in units of the bulk exciton Rydberg energy  $E_R$ , and

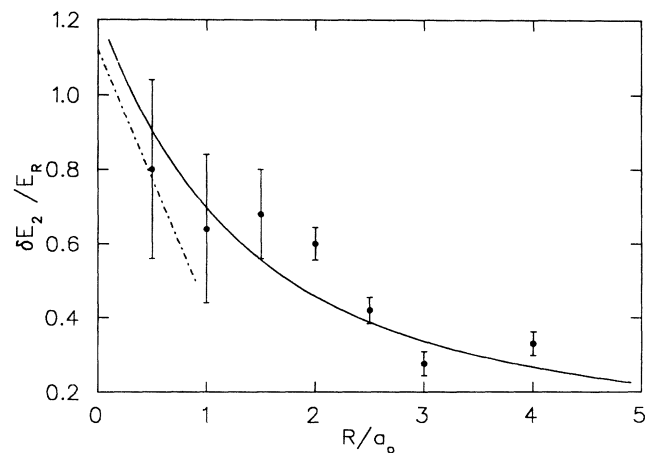


FIG. 1. Biexciton binding energy,  $\delta E_2/E_R$  [Eq. (1)], as function of quantum-dot radius  $R/a_0$ , where  $E_R$  and  $a_0$  are the bulk exciton binding energy and Bohr radius, respectively. The solid line shows the result of numerical matrix diagonalization; the dashed line is obtained from perturbation theory around  $R=0$ , Eq. (2), and the dots with the bars are quantum Monte Carlo results.

all lengths in units of the bulk exciton Bohr radius  $a_0$ . Third-order perturbation theory around  $R=0$  yields

$$\delta E_2/E_R = \Delta_1 - \Delta_2 R/a_0, \quad (2)$$

where  $\Delta_1$  and  $\Delta_2$  are given in terms of integrals over the exciton and biexciton wave functions. The evaluation of Eq. (2) is plotted as the dashed line in Fig. 1. In Ref. 5 it was shown that  $\Delta_1$  is strictly positive, independent of the system parameters, and we also find  $\Delta_2 > 0$ . The dots with the error bars in Fig. 1 have been obtained from quantum Monte Carlo calculations for excitons and biexcitons in quantum dots.<sup>6</sup> All these results show clearly that the biexciton binding energy increases with decreasing dot radius,  $R/a_0$ . For small quantum dots the biexciton binding energy is enhanced by more than an order of magnitude over the corresponding value in bulk semiconductors. The exact values of  $\delta E_2/E_R$  depend weakly on the mass ratio, but the overall functional variation is mass independent. Similar quantum-confinement enhanced biexciton ground-state energies have been reported also for quantum-well systems<sup>7-9</sup> and for quantum wires.<sup>10</sup>

Our matrix-diagonalization procedure yields the energies and wave functions not only for the exciton and biexciton ground state but also for all the excited states included in the basic sets. Using these wave functions we evaluate the various dipole matrix elements for transitions between the quantum-dot ground state and the one- and two-electron-hole-pair states. Inserting these results into the equation for the two-beam, third-order susceptibility, we calculate the changes in absorption  $\Delta\alpha$ , which should be seen in a pump-probe experiment.

Examples of the computed normalized transmission changes,  $-\Delta\alpha$ , are shown in Figs. 2(a)-2(c) for quantum dots with  $R/a_0=1.0$  and different homogeneous broadenings. These spectra are calculated for the case of resonant excitation of the energetically lowest exciton resonance, which in this case amounts to  $(\hbar\omega - E_g)/E_R = 6.2$ . The dominant feature in Figs. 2(a)-2(c) is the bleaching of the exciton state, causing the positive peak in the spectra. In addition to this exciton saturation, we see regions of increasing absorption (negative  $-\Delta\alpha$ ) which are the consequence of biexciton transitions. For the small homogeneous broadening  $\hbar\gamma = E_R$ , Fig. 2(a) shows induced probe absorption both below and above the exciton resonance. The absorption increase below the exciton resonance is due to the biexciton ground-state transition, reminiscent of results in bulk materials.<sup>1</sup> The additional induced absorption in the region around  $(\hbar\omega - E_g)/E_R \cong 12$  is due to the transition to excited biexciton states which are energetically between the two lowest exciton resonances. The dominant contribution to these transitions comes from biexcitons where the two electrons are in the  $1s$  state and the two holes are either both in the  $1p$  state, or one hole is in the  $1s$  and the other in the  $2s$  state, respectively. In Fig. 2(a) one can actual-

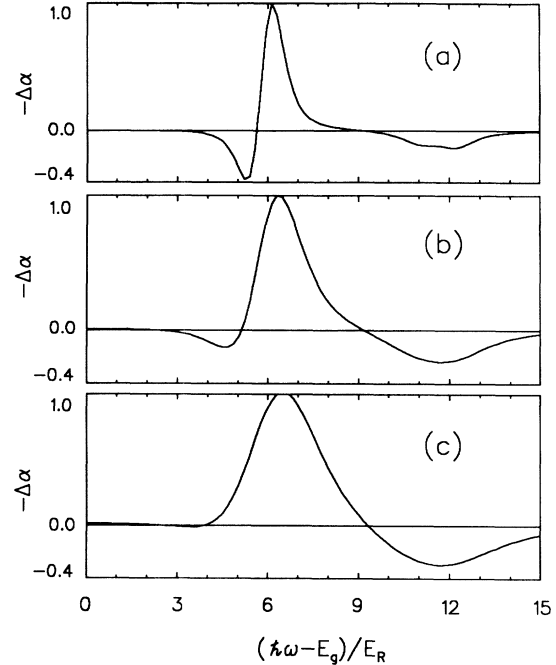


FIG. 2. Computed absorption change,  $-\Delta\alpha$ , for pump-probe excitation assuming pumping into the energetically lowest one-pair state. The parameters are  $m_e/m_h=0.24$ ,  $R/a_0=1$ , and (a)  $\hbar\gamma/E_R=1$ , (b) 2, and (c) 3, respectively.

ly identify both of these transitions as substructures in the increasing absorption regime around  $(\hbar\omega - E_g)/E_R \cong 11$  and 12. Such transitions would be dipole forbidden in the case without Coulomb interaction, and they are dipole allowed only because the Coulomb interaction breaks the symmetry of the quantum dots. This is the basic reason why these biexciton transitions are enhanced through the presence of impurities or defects.<sup>11</sup>

Increasing the homogeneous broadening to  $\hbar\gamma=2E_R$  [Fig. 2(b)] and  $\hbar\gamma=3E_R$  [Fig. 2(c)] shows that the biexciton ground-state transition is gradually suppressed by the dominating bleaching of the directly excited exciton resonance. However, the excited-state absorption on the high-energy side of the exciton resonance remains clearly resolved, since there is no competing one-photon resonance in this spectral regime.

For comparison with the theory, we have performed femtosecond and nanosecond pump-probe experiments on CdS and CdSe quantum dots in glass matrices. The results of our CdSe measurements are discussed in Refs. 11 and 12, where both the femtosecond and nanosecond experiments unambiguously show the predicted induced absorption features on the high-energy side of the bleached exciton resonance. For a direct comparison with the results in Fig. 2(c), we show in Fig. 3 our measurements for CdS quantum dots at 10 K. The pump pulse was tuned inside the energetically lowest exciton resonance and a broadband cross-polarized probe pulse

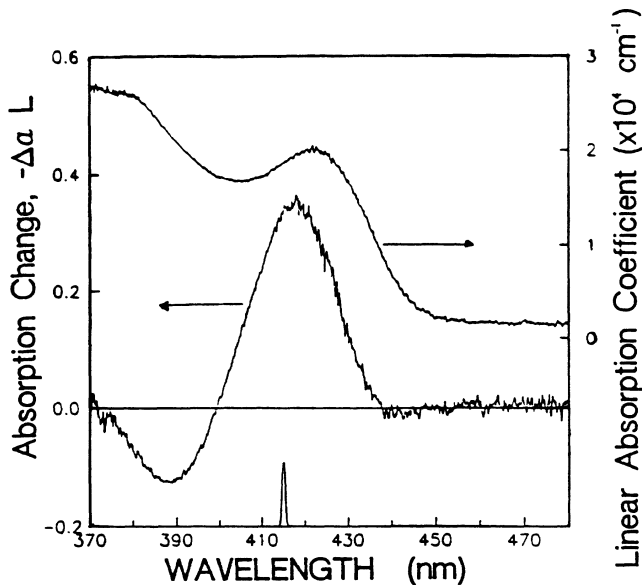


FIG. 3. Experimental results for CdS quantum dots in glass. The linear absorption spectrum is plotted together with the absorption changes and the spectral position of the pump.

measured the absorption changes induced by the pump. In addition to the absorption changes, we also show the linear absorption spectrum and the energetic position of the pump. The absorption changes clearly show the induced absorption feature on the high-energy side of the exciton transition, in good qualitative agreement with the theoretical predictions.

In conclusion, as a consequence of the Coulomb interaction, and as a unique quantum-confinement effect, we predict an increasing absorption due to excited biexciton states on the high-energy side of the exciton resonance. The only requirement for the observability of the predicted effects is the existence of reasonably well-defined quantum-confined resonances in the linear absorption spectra. The observation of the induced absorption in CdS quantum dots is shown and similar features have been seen also in other systems, such as CdSe or CdTe quantum dots in a glass matrix.

We appreciate receiving the samples for this study

from D. W. Hall and N. Borrelli at Corning Glass Works. The Arizona group would like to acknowledge support from NSF (Grants No. ECS8909913, No. ECS-8822305, and No. INT8713068 travel grant), ARO (Grant No. DAAL03-89-K-0100), NATO (travel Grants No. 86/0749 and No. 87/0736), ONR/Strategic Defense Initiative Organization (Grant No. N00014-86-K-0719), the Optical Circuitry Cooperative of the University of Arizona, and CPU time from the John von Neumann Computer Center. The work at Lawrence Livermore National Laboratory is performed under the auspices of the U.S. Department of Energy Contract No. W-7405-ENG-48.

<sup>1</sup>For reviews, see R. Levy, B. Hönerlage, and J. B. Grun, in *Optical Nonlinearities and Instabilities in Semiconductors*, edited by H. Haug (Academic, New York, 1988), p. 181; B. Hönerlage, R. Levy, J. B. Grun, C. Klingshirn, and K. Bohnert, *Phys. Rep.* **124**, 161 (1985).

<sup>2</sup>A. L. Efros and A. L. Efros, *Fiz. Tekh. Poluprovodn.* **16**, 1209 (1982) [*Sov. Phys. Semicond.* **16**, 772 (1982)].

<sup>3</sup>L. E. Brus, *J. Chem. Phys.* **80**, 4403 (1984); *IEEE J. Quantum Electron.* **22**, 1909 (1986).

<sup>4</sup>G. W. Bryant, *Phys. Rev. Lett.* **59**, 1140 (1987).

<sup>5</sup>L. Banyai, *Phys. Rev. B* **39**, 8022 (1989).

<sup>6</sup>In the quantum Monte Carlo calculations we numerically compute the density matrix of the exciton and biexciton system using path-integral methods. For a review see, e.g., E. L. Pollock and D. M. Ceperley, *Phys. Rev. B* **30**, 2555 (1984), and references therein. A detailed article on the quantum-dot path-integral calculations is in preparation.

<sup>7</sup>R. C. Miller, D. A. Kleinmann, A. C. Gossard, and O. Munteanu, *Phys. Rev. B* **25**, 6545 (1982).

<sup>8</sup>D. A. Kleinmann, *Phys. Rev. B* **28**, 871 (1983).

<sup>9</sup>Q. Fu, D. Lee, A. Mysyrowicz, A. V. Nurmikko, R. L. Gunshor, and L. A. Kolodziejcki, *Phys. Rev. B* **37**, 8791 (1988).

<sup>10</sup>L. Banyai, I. Galbraith, C. Ell, and H. Haug, *Phys. Rev. B* **36**, 6099 (1987).

<sup>11</sup>S. H. Park, R. A. Morgan, Y. Z. Hu, M. Lindberg, S. W. Koch, and N. Peyghambarian (to be published).

<sup>12</sup>N. Peyghambarian, B. Fluegel, D. Hulin, A. Migus, M. Joffre, A. Antonetti, S. W. Koch, and M. Lindberg, *IEEE J. Quantum Electron.* (to be published) (special issue on ultrafast phenomena).